Strojniški vestnik - Journal of Mechanical Engineering 53(2007)10, 635-656
UDK - UDC 531:622.673.6
Izvirni znanstveni članek - Original scientific paper (1.01)

Prenos vibracij preko prostorsko ukrivljenih jeklenih vrvi z oplaščenjem

The vibration over a spatially curved steel wire with an outer band

Miha Otrin[1,2] - Miha Boltežar[2]
([1]Cimos d.d., Koper; [2]Fakulteta za strojništvo, Ljubljana)

Prispevek obravnava študijo prenosa vibracij preko prostorsko ukrivljene jeklene vrvi z oplaščenjem. Fizikalni model upogibnih nihanj jeklene vrvi in oplaščenja je utemeljen na Euler-Bernoullijevem modelu upogiba nosilca brez upoštevanja osnih obremenitev. Disipacija energije je predstavljena v obliki dveh modelov, viskoznega in strukturnega modela disipacije energije. Frekvenčna odvisnost dinamičnega modula elastičnosti je identificirana iz meritev z uporabo prilagodne metode. Reševanje prenosa vibracij poteka numerično na podlagi končnih elementov z uporabo Newmarkove integracijske metode. Numerični model za jekleno vrv je vrednoten eksperimentalno. Med jekleno vrvjo in zunanjim oplaščenjem je obravnavan kontakt po kazenski metodi. Pri numeričnem preizkusu je analiziran vpliv zračnosti na velikost prenosa vibracij. Prikazana je možna uporaba mehanskega filtra za zmanjšanje prenosa vibracij preko jeklene vrvi.

(Ključne besede: prenos vibracij, jeklena žica, numerično modeliranje, disipacija energije)

This paper presents a study of the transmission of vibration over a spatially curved steel wire with an outer band. The physical model for the lateral vibrations of the steel wire and the outer band is based on the Euler-Bernoulli beam theory, with no axial preload. The dissipation of the energy is presented with two models: the viscous- and the structural-damping models. The frequency dependence of the dynamic modulus of elasticity is identified with an adaptive process. The vibration transmissibility was computed numerically on the basis of finite elements with the use of the Newmark integration scheme. The numerical model for the steel wire was validated experimentally. The penalty-contact model between the steel wire and the outer band was used. The numerical simulation for the influence of different gap values on the vibration transmission was made. The use of a mechanical filter to minimise vibration transmission is also demonstrated in numerical simulations.

(Keywords: vibration transmission, steel wire, numerical modeling, energy dissipation)

0 UVOD

Dandanes avtomobilska industrija zahteva od dobaviteljev vedno kakovostnejše izdelke, kar na vibracijskem področju lahko pomeni predvsem dvoje. Prvič, da je izdelek ustrezen z vidika trajnodinamične trdnosti, kar se običajno preverja s trajnodinamičnim testiranjem ter da je prenos vibracij prek elementov čim manjši, kar je običajno predmet numeričnih in eksperimentalnih analiz.

Ob zasnovi novih elementov ali sklopov za potrebe avtomobilske industrije, je običajno želja,

0 INTRODUCTION

Nowadays, the automotive industry demands, from its suppliers, better and better products, which from the vibration point of view means two things. Firstly, that the product is suitable in terms of vibration-related durability, which is mostly tested with a vibration durability test, and secondly, that the vibration transmission over the structural elements is as low as possible. Usually, this is analyzed with numerical and experimental processes.

In the design phase of a new product for the automotive industry, the focus is usually made (with

da bi izdelek ustrezal tako trajnodinamični trdnosti kakor tudi čim manjšim odzivnim lastnostim. Odzivna lastnost strukture je lahko povišana v primerih, ko je vzbujevalna frekvenca strukture v območju resonančnih področij strukture. Ker je pri zahtevnejših dinamičnih sistemih (osebni avtomobil) značilnost vzbujevalne motnje (neravno cestišče, delovanje motorja) praktično nemogoče spremeniti, se vzbujanju strukture v območju resonanc izognemo tako, da neželene resonance strukture s spremembo togostnih in masnih lastnosti "premaknemo" pod oziroma nad vzbujevalno frekvenco. Seveda ima takšen postopek uspehe predvsem v primerih, ko je vzbujevalna frekvenca konstantna. V primerih, ko vzbujevalna frekvenca ni konstantna (npr. naključno vzbujanje, vzbujanje s preletom vzbujevalnih frekvenc), pa se je težje izogniti vzbujanju v področju resonančnih frekvenc strukture. Odziv lahko v takšnih primerih zmanjšamo predvsem z dvema ukrepoma: s spremembo geometrijske oblike in materiala dinamične strukture v smeri večjih disipativnih lastnosti oziroma, kakor bomo v nadaljevanju pokazali, z uporabo t.i. mehanskega filtra. Izraz mehanski filter lahko razumemo kot ukrep, s katerim zmanjšamo odzivnost strukture po celotnem frekvenčnem območju vzbujanja oziroma preprečimo prekomerno odzivnost v območju resonanc.

V nadaljevanju se bomo osredotočili na obravnavo pretičnega mehanizma, ki je ena izmed neposrednih povezav med menjalnikom (motorjem) ter potniškim prostorom. Potnik je tako ob povečanem prenosu vibracij prek pretičnega mehanizma neposredno soočen s previsokimi amplitudami pomikov (pospeškov) prestavne ročice in armaturne plošče ter posledično hrupom, ki se zaradi vibracij elementov pretičnega mehanizma in medsebojnih trkov prenese v potniško kabino.

Pretični mehanizem je prikazan na sliki 1, kjer so tudi razvidni vplivnejši elementi pretičnega mehanizma. Kabel predstavlja jekleno vrv skupaj z gumenim oplaščenjem.

regard to vibrations) on the proper vibration durability and on a minimization of the response characteristic of the product. The response characteristic can be increased because the excitation frequency of the structure is in the resonance regions of that structure. In many cases the nature of the excitation cannot be changed (roadway, engine), so we are forced to modify the structure in a way that the positions of the resonances are changed (below or above the excitation frequency). This is usually made with a modification of the mass and the stiffness properties of the structure. It should be noted that this kind of intervention is successful when the excitation frequency is constant. When this is not the case; for example, in broadband or chirp excitation, the possible resonances are hard to avoid. In this case, the response can be lowered in two ways: firstly, with a change in the geometry of the dynamic structure, with the objective of larger dissipative capacities, or secondly, with the use of a mechanical filter, which will be discussed later in the paper. The term mechanical filter is used when describing the change in transmissibility when some mechanical structure is additionally applied to the observed system.

In the following we will concentrate on the gear-shift mechanism, which is one of the direct links between the engine gearbox and the passenger cabin. When the vibration transmission from the gearbox to the cabin is too high, the passenger is directly under the influence of the high displacement and acceleration amplitudes of the armature and the gear-shift handle. Consequently, the possible contact between structural elements of the gear-shift mechanism can also generate excessive noise, which is then transferred to the cabin.

The gear-shift mechanism is shown in Figure 1, where all the significant elements can be seen. The cable represents the steel wire together with a rubber outer band.

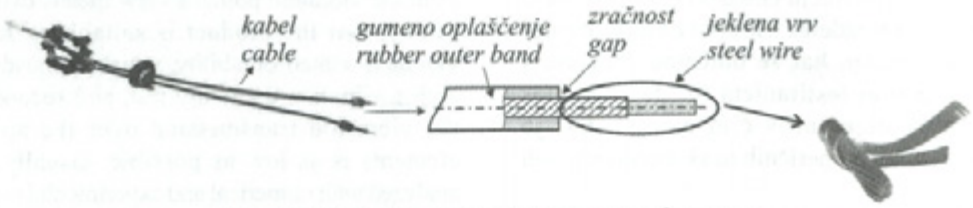

Sl. 1. *Vplivnejši elementi pretičnega mehanizma*
Fig. 1. *The main components of the gear-shift mechanism*

Vrv je konstrukcijski element, ki je običajno namenjen za prenos razmeroma velikih osnih obremenitev (npr. žični mostovi, žerjavi, ladjevje). V preteklosti je bilo narejenih veliko raziskav na področju popisa statičnega in dinamičnega obnašanja jeklenih vrvi. Costello [1] se pri raziskavah osredotoča predvsem na detajlno obravnavo posameznih vijačno ovitih žičk statično obremenjene jeklene vrvi. Nawrocki in Labrosse [2] sta izpeljala končni element ravne jeklene vrvi, ki se je pri vrednotenju pokazal kot primeren za popis dinamičnega obnašanja. Kar pa je skupno večini obravnav statičnega in dinamičnega obnašanja jeklenih vrvi, je to, da je glavna obremenitev osna obremenitev. V našem primeru je jeklena vrv osno neobremenjena ter je izpostavljena izključno upogibnim obremenitvam. Prav tako je osno neobremenjeno zunanje gumeno oplaščenje jeklene vrvi s prerezom kolobarja. Med vrvjo in oplaščenjem je zračnost, zaradi česar prihaja do medsebojnega kontakta.

Poleg numeričnega modeliranja (masna in togostna matrika), je popis disipacije energije pomemben del raziskav dinamičnega obnašanja struktur. V preteklosti je bilo razvitih veliko različnih modelov za popis disipacije energije ([3] in [4]), a vendar je velika pomanjkljivost njihova nesplošnost. Povedano drugače, disipacija je odvisna tako od materiala kakor od oblike strukture, zato je praktično nemogoče postaviti model, ki bi bil primeren za široko uporabo. V našem primeru smo se osredotočili na dva, v praksi največkrat uporabljena modela, in sicer proporcionalni model viskoznega dušenja in model strukturnega dušenja ([6] in [7]).

Namen prispevka je pokazati numerični model napovedi dinamičnega obnašanja jeklene vrvi z oplaščenjem. V prvem poglavju je predstavljen numerični model jeklene vrvi in oplaščenja. V drugem poglavju so identificirani bistveni parametri modela. V tretjem poglavju je predstavljena veljavnost numeričnega modela. Ker med vzbujanjem jeklene vrvi in oplaščenja prihaja do medsebojne interakcije, je v ta namen v četrtem poglavju predstavljen kontaktni model brez trenja. Zračnost med jekleno vrvjo in oplaščenjem pomembno vpliva na odziv sistema, zato je v petem poglavju predstavljen vpliv nekaterih parametrov kontakta na odziv sistema. Analizirana je jeklena vrv z oplaščenjem, predstavljen pa je tudi primer uporabe mehanskega filtra za

The steel wire represents an element that is usually meant to withstand relatively large axial forces (e.g., bridges, cranes, and shipbuilding yards). In recent years many studies have been made in the field of modelling the static and the dynamic behaviour of the steel wires. Costello [1] has focused his research on a detailed study of the helically curved wires in one steel wire block. Nawrocki and Labrosse [2] have made their research in the field of developing the finite element of a straight wire, also based on a detailed consideration of the wire's geometry. They have also made a validation of their numerical model, which has proved to be reliable. A common feature of most research is that the axial load is the main loading on the steel wire under consideration. In our case, the steel wire has no pre-stress in the axial direction, so the wire is exposed only to the bending vibrations. The same characteristic applies to the rubber, outer band. Between the wire and the band a contact can arise, as we will see later.

Beside the numerical modelling (the mass and stiffness matrix), the derivation of the dissipation function is very important for a proper evaluation of the dynamic behaviour of the structure. Many damping models have been developed over the years ([3] and [4]), but the main deficiency is still that they can only be made valid for specific types of structure. In other words, the dissipation function depends on the material and the shape of the structure, so it is practically impossible to derive a model that will be suitable for a broad range of problems. In our case, two different models are considered in the numerical modelling, i.e., the proportional viscous damping model and the structural damping model ([6] and [7]).

The main contribution of this paper is to present a numerical model for the prediction of the dynamic behaviour of a steel wire with a rubber outer band. In the first section the numerical model of the steel wire and outer band is derived. In second section, the main material parameters are identified. The validation of the model will be described in the third section. Because during the movement of the steel wire and the outer band a possible contact can arise, the contact model will be derived in the fourth section. The gap between the wire and the outer band significantly influences the dynamic behaviour of the system, so the numerical simulation of the system with different values of parameters will be given in the fifth section. The curved steel wire with the outer band will be

zmanjšanje prenosa vibracij oziroma za zmanjšanje resonančnih vrhov jeklene vrvi. Zadnje poglavje je namenjeno sklepom.

Podrobna raziskava prenosa vibracij preko osno neobremenjene jeklene vrvi je objavljena v [5], zato je prikaz v prvih dveh poglavjih (numerični model in identifikacija parametrov) namenjen zgolj celovitosti tega prispevka.

1 MODEL JEKLENE VRVI IN OPLAŠČENJA

Jeklena vrv (v nadaljevanju - vrv) in gumeno oplaščenje (v nadaljevanju – oplaščenje) sta v osni smeri neobremenjena. Prenos vibracij po poljubno ukrivljenih vrveh in oplaščenja smo obravnavali po Euler-Bernoullijevi teoriji upogibnega nosilca, brez upoštevanja osne sile. Fizikalni model je enak tako za vrv kakor za oplaščenje in je prikazan na sliki 2. Model je diskretiziran s končnimi elementi, analizo dinamičnega obnašanja pa smo izvajali numerično.

Poleg znanih predpostavk Euler-Bernoullijeve formulacije upogiba nosilca smo predpostavili še homogenost materiala ter nepovezanost pomikov in zasukov. Togostno matriko $\mathbf{k}_i$ in masno matriko $\mathbf{m}_i$ vrvi oziroma oplaščenja lahko zapišemo po enačbi (1), kjer indeks pomeni i-ti končni element.

$$\mathbf{k}_i = \mathbf{B}^{\mathrm{T}}\mathbf{D}\mathbf{B}\mathrm{d}V, \quad i=1...N$$
$$\mathbf{m}_i = \mathbf{N}^{\mathrm{T}}\rho\mathbf{N}\mathrm{d}V, \quad i=1...N \qquad (1),$$

pri čemer so matrika **B** povezava deformacija - pomik, matrika **D** povezava deformacija - napetost, **N** matrika interpolacijskih polinomov, ρ gostota materiala infinitezimalnega delčka dV ter N število vseh končnih elementov sistema. Ker je lahko geometrijska oblika vrvi in oplaščenja poljubno ukrivljena v prostoru, je treba določiti

analyzed. An example of using the mechanical filter for minimizing the transmission of vibration will also be shown. The last section contains the conclusions.

A detailed analysis of the transmission of vibration over the steel wire with no axial pre-load is shown in [5]. For the sake of completeness, the first two sections will give a brief review of this analysis.

1 DYNAMIC MODEL OF A STEEL WIRE AND AN OUTER BAND

The steel wire (subsequently referred to as the wire) and rubber outer band (subsequently referred to as the band) are without axial pre-load. The Euler-Bernoully beam theory with no axial pre-load was used for the derivation of the finite-element matrices. The physical model is the same for the wire and the band, and it is shown in Figure 2. The model is discretized with the finite elements, so the computation was done numerically.

Besides the well-known assumption of the Euler-Bernoully model for a beam deflection some additional assumptions were made: the materials of the wire and band are homogeneous and the displacements and rotations are uncoupled. The stiffness matrix $\mathbf{k}_i$ and the mass matrix $\mathbf{m}_i$ of the wire and band can be written with Equation (1), where the index i represents the i-th finite element.

The matrix **B** is the strain-displacement matrix, **D** is the stress-strain matrix, **N** is the interpolation polynomials matrix, ρ is the density of the material of the infinitesimal part dV and N is the number of finite elements in the system. Because the geometry of the wire and the band can be arbitrarily curved in space, the proper transformation matrix $\mathbf{T}_i$ of each

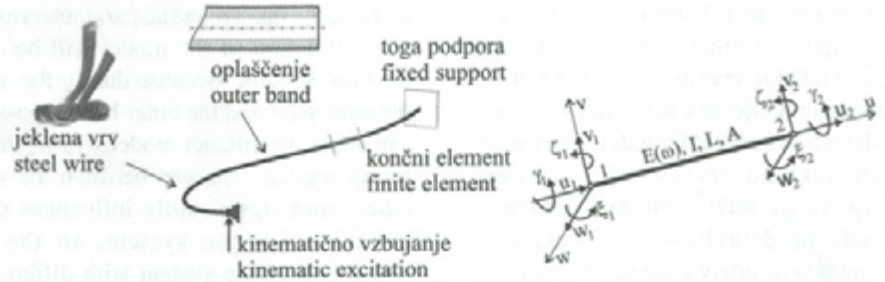

Sl. 2. *Fizikalni model jeklene vrvi in oplaščenja; uporabljen končni element*
Fig. 2. *Physical model for the steel wire and the outer band; the finite element used*

transformacijsko matriko $\mathbf{T}_i$ posameznega končnega elementa. Le-ta je dobljena z uporabo Eulerjevih kotov, ki enolično določajo zavrtitev lokalnega koordinatnega sistema končnega elementa v skupnem koordinatnem sistemu. Ob poznavanju matrike $\mathbf{T}_i$, lahko torej zapišemo matriki kot:

finite element must be derived. The transformation matrix can be computed on the basis of the Euler angles, which define the rotation of the local coordinate system relative to the global coordinate system. With the known $\mathbf{T}_i$ matrix the global stiffness and mass matrix are:

$$\mathbf{K}_i = \mathbf{T}_i^T \mathbf{k}_i \mathbf{T}_i$$
$$\mathbf{M}_i = \mathbf{T}_i^T \mathbf{m}_i \mathbf{T}_i \quad (2).$$

Pri postavitvi gibalnih enačb smo se omejili na dva modela disipacije energije, in sicer proporcionalni viskozni model, enačba (3) in strukturni model, enačba (4).

When defining the dynamic equation, two damping models were used, i.e., the proportional viscous damping model, Equation (3), and the structural damping model, Equation (4).

$$\mathbf{M}\ddot{\mathbf{q}}_v(t) + \mathbf{C}\dot{\mathbf{q}}_v(t) + \mathbf{K}\mathbf{q}_v(t) = \mathbf{F}_v e^{i\omega t} \quad (3)$$

$$\mathbf{M}\ddot{\mathbf{q}}_s(t) + (1+i\eta)\mathbf{K}\mathbf{q}_s(t) = \mathbf{F}_s e^{i\omega t} \quad (4),$$

kjer **M**, **K** in **C** pomenijo sistemsko masno, togostno in dušilno matriko sistema, η pomeni koeficient izgub, $\mathbf{F}_v$ in $\mathbf{F}_s$ pa sta vektorja zunanjih vozliščnih obremenitev. V enačbi (3) in (4) ter v nadaljevanju se indeks *v* navezuje na viskozni model, indeks *s* pa na strukturni model disipacije energije.

where **M**, **K** and **C** represent the system mass, stiffness and damping matrix, respectively, η represents the loss factor and the $\mathbf{F}_v$ and $\mathbf{F}_s$ vectors represent the external forces on the system. In Equations (3) and (4), and also in the subsequent text, the index *v* corresponds to the viscous-damping model and the index *s* to the structural damping model.

Vzbujevalna motnja je vnešena v obliki kinematičnega pomika podpore (sl. 1), zato je smotrno sistemske matrike **M**, **K** in **C** razstaviti na znane in neznane vrednosti spremenljivk v vozliščih elementa. V primeru obravnave dinamičnega odziva vrvi in oplaščenja lahko ločeno (brez medsebojne interakcije) ustaljeno stanje določimo z uvedbo nastavka za rešitev oblike:

The excitation of the system is applied with the kinematic movement of the support end, Figure 1, so the partitioning of the **M**, **K** and **C** matrices to known and unknown node values was applied. In the case when there is no interaction between the wire and the band the steady-state solution can be derived, if the solution is in the form:

$$\mathbf{q}(t) = \mathbf{X}e^{i(\omega t+\varphi)} \quad (5).$$

Z upoštevanjem viskoznega modela disipacije energije lahko gibalno enačbo zapišemo v obliki:

With the use of the viscous-damping model, the equation of motion can be written in the form:

$$\left(-\omega^2\begin{bmatrix}\mathbf{M}_{vv} & \mathbf{M}_{vp}\\ \mathbf{M}_{pv} & \mathbf{M}_{pp}\end{bmatrix} + i\omega\begin{bmatrix}\mathbf{C}_{vv} & \mathbf{C}_{vp}\\ \mathbf{C}_{pv} & \mathbf{C}_{pp}\end{bmatrix} + \begin{bmatrix}\mathbf{K}_{vv} & \mathbf{K}_{vp}\\ \mathbf{K}_{pv} & \mathbf{K}_{pp}\end{bmatrix}\right)\begin{pmatrix}\mathbf{X}_v\\ \mathbf{X}_p\end{pmatrix} = \begin{pmatrix}\mathbf{F}_v\\ \mathbf{F}_p\end{pmatrix} \quad (6),$$

ter z upoštevanjem strukturnega modela disipacije v obliki:

and when the structural-damping model is applied, the equation of motion is in the form:

$$\left(-\omega^2\begin{bmatrix}\mathbf{M}_{ss} & \mathbf{M}_{sp}\\ \mathbf{M}_{ps} & \mathbf{M}_{pp}\end{bmatrix} + (1+i\eta)\begin{bmatrix}\mathbf{K}_{ss} & \mathbf{K}_{sp}\\ \mathbf{K}_{ps} & \mathbf{K}_{pp}\end{bmatrix}\right)\begin{pmatrix}\mathbf{X}_s\\ \mathbf{X}_p\end{pmatrix} = \begin{pmatrix}\mathbf{F}_s\\ \mathbf{F}_p\end{pmatrix} \quad (7).$$

Iz enačb (6) in (7) lahko izrazimo enačbo prenosnosti v obliki funkcije:

From Equations (6) and (7) the transmissibility function can be obtained as:

$$\mathrm{TRFAM}(\omega_i) = \frac{F_{p(i)}}{X_{p(i)}} \quad (8),$$

kjer $F_{p(i)}$ pomeni amplitudo sile v podpori, $X_{p(i)}$ pa amplitudo prečnega vzbujevalnega pomika pri

where $F_{p(i)}$ represents the support-force amplitude, and $X_{p(i)}$ the displacement amplitude of the support

diskretni krožni frekvenci ω_i. Kratica TRFAM označuje prenosno funkcijo v obliki navidezne mase.

2 IDENTIFIKACIJA PARAMETROV

V splošnem je identifikacija parametrov posledica nepoznavanja predvsem materialnih lastnosti obravnavane strukture. Za vrv smo identificirali parametre, ki se navezujejo na popis disipacije energije, ter dinamični modul elastičnosti. Za oplaščenje smo razpoznali zgolj dinamični modul elastičnosti, saj bo numerični model oplaščenja uporabljen samo pri numerični analizi interakcije med vrvjo in oplaščenjem.

2.1 Parametri disipacije energije

Za popis disipacije energije smo uporabili (*i*) proporcionalni model viskoznega dušenja, pri čemer je dušilna matrika dobljena na osnovi Rayleighovih koeficientov in (*ii*) strukturni model dušenja, z upoštevanjem kompleksne togosti.

2.1.1 Viskozni model disipacije energije

Rayleighov model predpostavlja, da je matrika dušenja proporcionalna z masno in togostno matriko kot:

$$\mathbf{C} = \alpha\mathbf{M} + \beta\mathbf{K} \tag{9},$$

pri čemer je treba identificirati koeficienta α in β. Zapišemo lahko razmerje:

$$\begin{bmatrix} \tilde{\zeta}_1 \\ \tilde{\zeta}_2 \\ \vdots \\ \tilde{\zeta}_m \end{bmatrix} = \begin{bmatrix} \dfrac{1}{2\tilde{\omega}_1} & \dfrac{\tilde{\omega}_1}{2} \\ \dfrac{1}{2\tilde{\omega}_2} & \dfrac{\tilde{\omega}_2}{2} \\ \vdots & \vdots \\ \dfrac{1}{2\tilde{\omega}_m} & \dfrac{\tilde{\omega}_m}{2} \end{bmatrix} \begin{bmatrix} \alpha \\ \beta \end{bmatrix} \tag{10},$$

kjer sta $\tilde{\omega}_m$ m-ta izmerjena lastna frekvenca jeklene vrvi in $\tilde{\zeta}_m$ m-ti identificirani razmernik dušenja. Vrednosti omenjenih parametrov smo določili iz opravljenih meritev po metodi identifikacije parametrov z uporabno metode najmanjših

excitation at the discrete excitation frequency ω_i. The abbreviation TRFAM is used for the term transfer function in terms of the apparent mass.

2 PARAMETER IDENTIFICATION

In general, the parameter identification is the result of a lack of knowledge about the material characteristics of the dynamic system. For the wire, the damping parameters and the frequency dependence of the dynamic modulus of elasticity were identified, and for the band only the frequency dependence of the dynamic modulus of elasticity was identified. The reason for this is that the band model will only be used in numerical simulations, so no prior validation of the band model was made.

2.1 The Dissipative Parameters

Two different damping models were used for the derivation of the energy dissipation: (*i*) the viscous-damping model, where the damping matrix is written in the form of Rayleigh coefficients and (*ii*) the structural-damping model, where the complex stiffness of the matrix is introduced.

2.1.1 Viscous-Damping Model

The Rayleigh damping model assumes that the damping matrix is proportional to the mass and stiffness matrix with the relation:

$$\mathbf{C} = \alpha\mathbf{M} + \beta\mathbf{K} \tag{9},$$

where the coefficients α and β need to be identified. We can write the relation:

$$\begin{bmatrix} \tilde{\zeta}_1 \\ \tilde{\zeta}_2 \\ \vdots \\ \tilde{\zeta}_m \end{bmatrix} = \begin{bmatrix} \dfrac{1}{2\tilde{\omega}_1} & \dfrac{\tilde{\omega}_1}{2} \\ \dfrac{1}{2\tilde{\omega}_2} & \dfrac{\tilde{\omega}_2}{2} \\ \vdots & \vdots \\ \dfrac{1}{2\tilde{\omega}_m} & \dfrac{\tilde{\omega}_m}{2} \end{bmatrix} \begin{bmatrix} \alpha \\ \beta \end{bmatrix} \tag{10},$$

where $\tilde{\omega}_m$ represents the m-th measured natural frequencies of the wire and $\tilde{\zeta}_m$ the m-th identified damping ratio from the measurement. The values of the mentioned parameters were identified with the use of the least-squares method, adopted by

kvadratov [9]. Enačbo (10) lahko zapišemo v poenostavljeni matrični obliki:

[9]. Equation (10) can be rewritten in a simplified form:

$$\mathbf{Z}=\mathbf{AR} \tag{11}.$$

S posplošenim obratom lahko iz enačbe (11) določimo vrednosti matrike **R**, ki predstavlja vrednosti parametrov α in β:

With the help of the *pseudo-inverse* routine, the unknown matrix **R** can be calculated. The matrix **R** represents the α and β factor, and can be calculated with:

$$\mathbf{R}=\mathbf{A}^{+}\mathbf{Z} \tag{12},$$

kjer $\mathbf{A}^{+}$ pomeni nepravo obratno matriko **A**.

where $\mathbf{A}^{+}$ represents the pseudo-inverse of matrix **A**.

2.1.2 Strukturni model disipacije energije

Iz enačbe (7) je razvidno, da je v primeru upoštevanja strukturnega dušenja treba identificirati koeficient izgub. Za linearne sisteme se izkaže, da meritev TRFAM v okolici lastnih frekvenc, v Nyquistovem diagramu apoksimira obliko krožnice [8]. Izmerjenim vrednostim TRFAM lahko torej v primeru linearnih sistemov aproksimiramo analitično krožno funkcijo, iz česar poleg lastne frekvence ω_0 določimo še obe mejni frekvenci ω_1, ω_2. Postopek identifikacije koeficienta izgub je s primerom prikazan na sliki 3. Ob poznavanju omenjenih frekvenc lahko faktor izgub *m*-te lastne frekvence določimo po enačbi (13):

2.1.2 Structural-Damping Model

It is clear from Equation (7) that in the case of the structural-damping model, the loss factor needs to be identified. It turns out (for linear systems) that the TRFAM measurement in the resonance region in the Nyquist plot produces an approximation to a circle [8]. The measured TRFAM values can then be approximated to an analytical function, from which the natural frequency ω_0 and the boundary frequencies ω_1, ω_2 can be identified. An example of such a routine is shown in Figure 3. When the mentioned frequencies are known, the *k*-th loss factor can be computed for the *m*-th natural frequency, Equation (13):

$$\eta_{(k)}=\frac{\omega_{2(m)}^2-\omega_{1(m)}^2}{2\omega_{0(m)}^2} \tag{13}.$$

2.1.3 Dinamični modul elastičnosti

Kakor je bilo že omenjeno, smo frekvenčno odvisnost dinamičnega modula identificirali tako za vrv kakor oplaščenje. Frekvenčno odvisnost smo v obeh primerih identificirali z uporabo prilagoditvene metode. Metoda sloni na prilagajanju lastnih

2.1.3 Dynamic Modulus Of Elasticity

As was previously mentioned, the frequency dependence of the dynamic modulus of elasticity was identified for both the wire and the band system. We identified the proper curve with an adaptive process. The basic idea of the process is

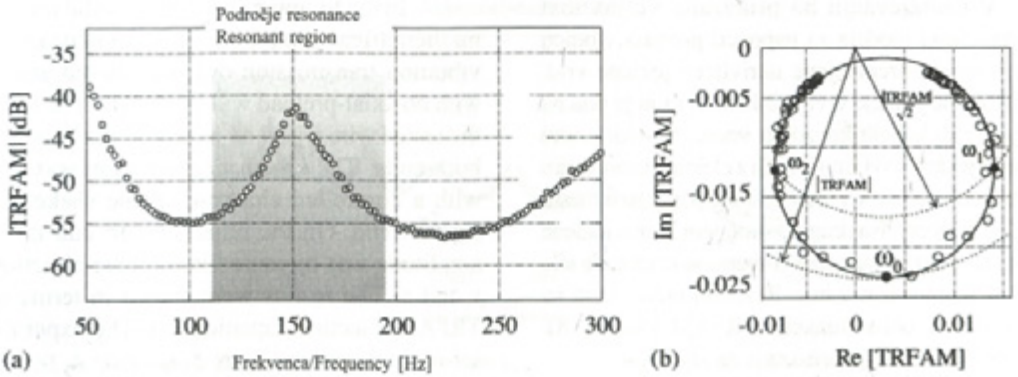

Sl. 3. *(a) Bodejev diagram, (b) Nyquistov diagram*
Fig. 3. *(a) Bode diagram, (b) Nyquist diagram*

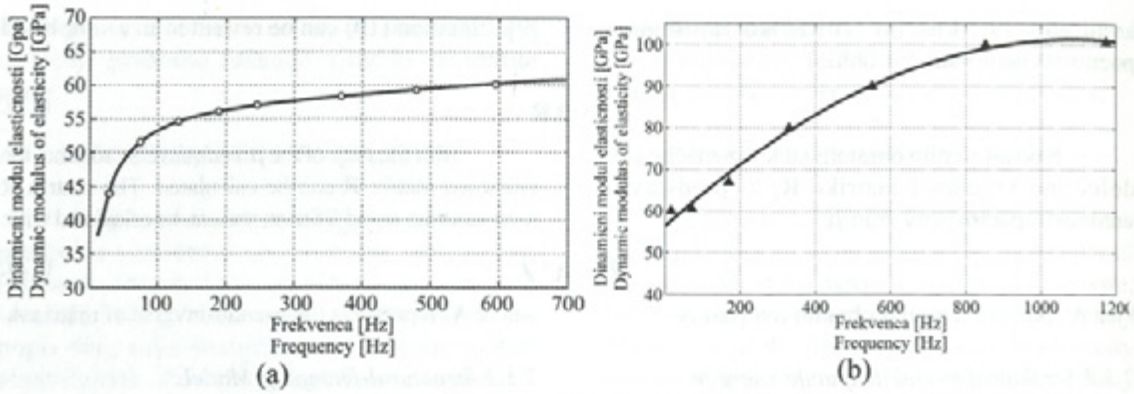

Sl. 4. *Frekvenčna odvisnost dinamičnega modula elastičnosti: (a) jeklena vrv, (b) oplaščenje*
Fig. 4. *Frequency dependence of the dynamic modulus of elasticity: (a) wire, (b) band*

frekvenc jeklene vrvi, dobljenih iz matematičnega modela, izmerjenim vrednostim lastnih frekvenc. Graf frekvenčne odvisnosti dinamičnega modula elastičnosti vrvi in oplaščenja je prikazan na sliki 4.

2.1.4 Geometrijski in materialni podatki

Geometrijski in materialni podatki za vrv in oplaščenje so podani v preglednici 1.

that the numerically derived natural frequencies are adapted with the measured ones. The curve that represents the frequency dependence of the dynamic modulus of elasticity is shown in Figure 4.

2.1.4 Geometrical And Material Data

The material and geometrical properties of the wire and the band are listed in Table 1.

Preglednica 1. *Geometrijski in materialni podatki za vrv in oplaščenje*
Table 1. *Geometrical and material data for the wire and the band*

	Jeklena vrv – steel wire	*Oplaščenje – outer band*
D_Z [m]	*0,0032*	*0,0095*
D_N [m]	/	*0,0035*
I [m^4]	$3{,}1083\,10^{-12}$	$3{,}9245\,10^{-10}$
ρ [kg/m^3]	*7650*	*4535*

$_Z$ – *zunanji premer, outer diameter,* $_N$ – *notranji premer, inner diameter*

3 VELJAVNOST MODELA

V nadaljevanju bo prikazana veljavnost matematičnega modela za napoved prenosa vibracij preko osno neobremenjene ukrivljene jeklene vrvi. Dolžina testne jeklene vrvi je bila *0,68* m in je bila na obeh skrajnih koncih konzolno vpeta. Nadzorovano vzbujanje jeklene vrvi smo izvedli z elektro-dinamičnim stresalnikom, s točko vnosa amplitude pomika na mestu konzolne podpore. Na drugem skrajnem koncu jeklene vrvi je bila v konzolni podpori merjena amplituda sile v vseh treh smereh *x*, *y* in *z*. Rezultati prenosnosti so predstavljeni v obliki funkcije TRFAM, enačba (8). Postavitev preizkusa je prikazana na sliki 5(a).

Rezultati identifikacije parametrov razmernikov dušenja, Rayleighovih koeficientov in

3 VALIDATION OF THE MODEL

In the following section the validation of the mathematical model for the calculation of the vibration transmission over the curved steel wire with no axial-preload will be shown. The length of the tested wire was *0.68* m, and it was supported at both ends. The kinematic excitation was applied with a controlled electro-dynamic shaker at one support end. On the other support end the force amplitude was measured in all three directions: *x*, *y* and *z*. The results were shown in terms of the TRFAM function Equation (8). The experimental set-up is shown in Figure 5(a).

The results of the identified damping ratios, the Rayleigh coefficients and the frequency

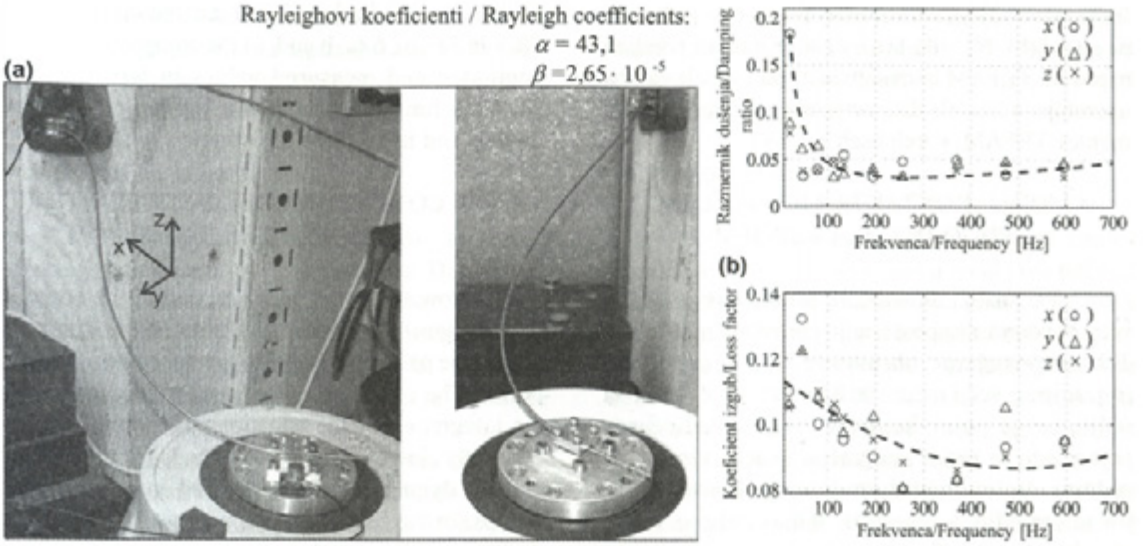

Sl. 5. *Lega ukrivljene jeklene vrvi v prostoru, (b) identificirani razmerniki dušenja in koeficienti izgub*
Fig. 5. *The geometry of the wire in space, (b) identified damping ratios and loss factors*

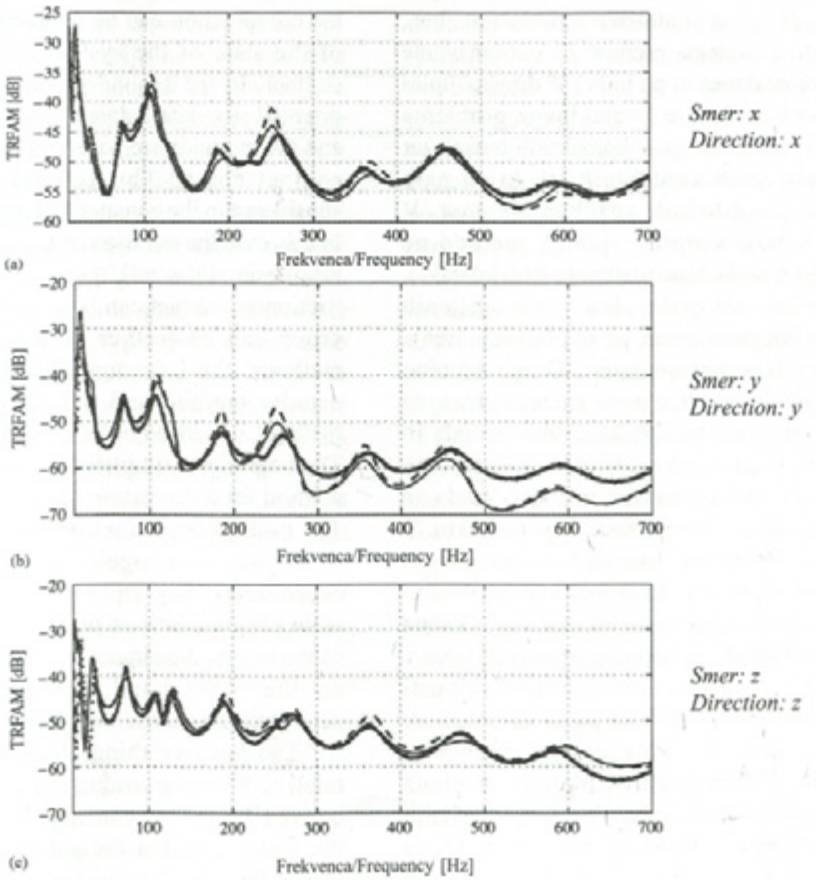

Sl. 6. *Veljavnost prenosa vibracij: (○) meritev, (—) strukturni model, (---) viskozni model*
Fig. 6. *Validation of the vibration transmission: : (○) measurement, (—) structural model, (---) viscous model*

frekvenčne odvisnosti koeficienta izgub so prikazani na sliki 5(b). Na sliki 6(a,b,c) so prikazani rezultati napovedi TRFAM iz matematičnega modela za oba uporabljena modela disipacije energije ter rezultati meritev TRFAM, v treh oseh *x*, *y* in *z*.

4 MODEL KONTAKTA MED JEKLENO VRVJO IN OPLAŠČENJEM

Pri analizi dinamičnih problemov je vedno večji poudarek na upoštevanju kontaktov med telesi. Takšno povečanje obravnave kontaktov lahko pripisujemo večji računalniški moči, ki je danes na voljo, saj je pojav kontakta izrazito nelinearen pojav, zato je lahko integracija enačb razmeroma počasna. Večino metod modeliranja kontaktov, ki jih je zaslediti v literaturi, lahko delimo v dve skupini. V prvi skupini reševanje kontaktnega problema temelji na upoštevanju zakona o ohranitvi gibalne količine (običajen trk). Za takšen postopek je značilno, da je čas kontakta neskončno majhen, tako se analiza kontakta prenese na obravnavanje stanja pred kontaktom in po njem. V drugi skupini pa metode za reševanje kontaktnega problema temeljijo na analizi stanja v kontaktnih točkah ter določitvi ustreznih kontaktnih sil, ki so nato upoštevane pri gibalnih enačbah sistema. V nasprotju s prvo skupino slednje metode ne predpostavljajo neskončno majhnega časa kontakta, kar posledično omogoča obravnavo lepljenih kontaktov v normalni smeri ter upoštevanja trenja v kontaktu v tangencialni smeri. Drugo skupino lahko delimo še na tri glavne metode: metoda Lagrangeovih množilnikov, kazenska metoda in povečevalna Lagrangeova metoda, ki združuje lastnosti prvih dveh omenjenih metod. Metoda na podlagi Lagrangeovih množilnikov je kontaktu. V gibalno enačbo vpeljani Lagrangeovi množilniki pomenijo kontaktne sile, ki skupaj s posplošenimi koordinatami pomenijo neznanke sistema. Glavna značilnost te metode je neprodiranje dveh teles v kontaktu. Kazenska metoda v osnovi dopusti prodiranje dveh teles, globina pa je za določitev sile v kontaktu pomnožena s kazenskim parametrom. Dobra lastnost metode je njena razmeroma preprosta uporaba v že znanih modelih končnih elementov. Slabi lastnosti metode sta predvsem: odvisnost rešitve od vrednosti kazenskega parametra ter kršenje zakona o ohranitvi energije teles v kontaktu, saj se del energije shrani v t.i. kontaktni kazenski vzmeti.

dependence of the loss factor are shown in Figure 5(b). In Figure 6 (a, b and c) the comparison of the computed and measured values in terms of the TRFAM function are shown for both damping models and in all three directions: *x*, *y* and *z*.

4 THE CONTACT MODEL BETWEEN THE WIRE AND THE BAND

Nowadays, the consideration of the contact in a dynamic analysis plays a much greater role than in the past, mainly due to greater computational power. The contact is a nonlinear phenomenon, so the integration of the equations of motion can be relatively slow. Most of the methods for modelling contact dynamics can be divided into two main groups. In the first group the computation is made on the basis of impulse-momentum methods. For this kind of contact modelling the duration of the contact is assumed to be infinitesimally small so the computation can be transferred to the analysis of the state of the system before and after the contact. In the second group the computation is oriented to a detailed analysis of the contact phase and the methods are based on the derivation of the contact force. The contact forces are then considered in the equations of motion of the system. In this case the duration of the contact phase is not infinitesimally small, so the stick phases and the friction in contact can be considered. The second group can be further divided into three main methods: the Lagrange multipliers method, the penalty method and the augmented Lagrange method, which combines the first two methods. The Lagrange multipliers method is the most exact method for a derivation of the contact conditions. The multipliers are introduced into the equation of motion, and together with the generalized coordinates they represent the unknowns. The main characteristic is that there is no penetration of the two bodies in contact. The penalty method, on the other hand, assumes a small-body penetration, because the contact force depends on it. The positive thing about this method is its relatively easy introduction into the previously derived finite-element models. The drawback of the method is that the solution depends on the value of the penalty parameter, and that the method violates the energy-conservation-law phase, because some energy is stored in the so-called penalty spring.

V pričujočem prispevku bo za popis kontaktnega problema uporabljena kazenska metoda, in sicer brez upoštevanja trenja v tangencialni smeri kontakta.

4.1 Kazenska metoda

Obravnavamo s končnimi elementi diskretiziran sistem vrvi in oplaščenja. Definiramo mejo vozliščnih točk φ sistema vrvi β kot $\varphi(\beta^1)$ ter oplaščenja kot $\varphi(\beta^2)$ (sl. 7). Opazovani točki na meji obeh teles sta vektorja pomika $\mathbf{X}^1$ in $\mathbf{X}^2$. Pri času *t* točki teoretično prideta v kontakt, ko je izpolnjen pogoj $\varphi(\mathbf{X}^1,t) = \varphi(\mathbf{X}^2,t)$ [10].

Pri kazenski metodi je kontaktna sila poleg velikosti kazenskega parametra odvisna tudi od globine prodiranja, zato je pravilna določitev le-te zelo pomembna. Usmerjenost in velikost vektorja prodiranja je določena z vektorjem normale v kontaktni točki. Ločimo dva primera določitve vektorja normale v kontaktu. V prvem primeru (sl. 8(a)), je kontakt definiran izključno na vozliščnem paru, tako da je normala kontakta kar povezujoča črta vozlišč v kontaktu. Takšna določitev normale in posledično usmerjenost kontaktne sile vodi k nenatančnemu popisu mesta kontakta. V drugem primeru (sl. 8(b)) najprej izberemo vodilno telo β^1, katerega vozlišča v normalni smeri določajo mesto kontakta na meji telesa $\varphi(\beta^2)$. V takšnem primeru so mesto kontakta, velikost in smer kontaktne sile bolj natančno določeni. V prispevku smo zato uporabili slednji postopek. Število mogočih sočasnih kontaktnih točk je v primeru diskretizacije telesa s končnimi elementi odvisno od števila vozliščnih točk na meji telesa β^1, če je le-to telo vodilno. Vodilno telo bomo v nadaljevanju poimenovali prodirno telo, telo v kontaktnem paru pa predrto telo.

Prodirno funkcijo, ki definira velikost prodiranja v kontaktu, lahko pri kazenski metodi, navezujoč se na sliko 8(b), zapišemo kot:

In this paper the penalty method is used for analyzing the contact problem. The contact is assumed to have no friction in the tangential direction of the contact.

4.1 Penalty Method

We are analyzing the discretized finite-element system of a wire and a band. We defined the boundary of the node points as φ, of the wire body β as $\varphi(\beta^1)$, and for the band as $\varphi(\beta^2)$, Figure 7. The vectors of the potential contact points are denoted with $\mathbf{X}^1$ and $\mathbf{X}^2$. In time *t*, two points theoretically come into contact when the condition $\varphi(\mathbf{X}^1,t) = \varphi(\mathbf{X}^2,t)$ is realized [10].

In the penalty method the contact force depends on the value of the penalty parameter and on the size of the penetration of the two bodies, so the proper contact point and the proper direction of the contact penetration is very important. The direction and size of the penetration is defined with the normal vector in the contact point. We can define two cases for defining the normal vector. In the first case, Figure 8(a), the contact is defined only by a node-to-node contact, so the direction of the normal vector is naturally defined with the position of the nodes in contact. The normal derived in this way can lead to an improper direction of the contact normal vector. In the second case, Figure 8(b), the master body β^1 is assigned first and the nodal points of the master body in the normal direction give the possible contact points of the slave body $\varphi(\beta^2)$, regardless of the slave-body nodal discretization. In this case the direction of the contact normal is more precise. In this paper we used the latter method. The number of possible simultaneous contact points is defined by the discretization of the boundary of the master body β^1.

The penetration function, which defined the value of the contact penetration, can be, in the case of the penalty method, Figure 8(b), defined as:

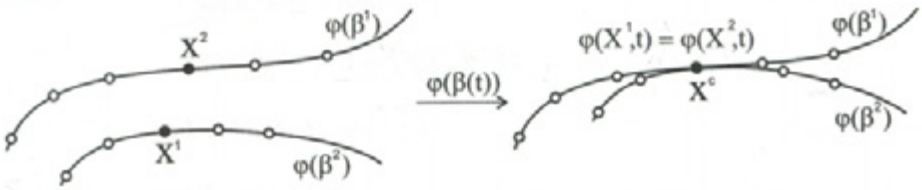

Sl. 7. *Geometrijska oblika kontakta*
Fig. 7. *Definition of the contact geometry*

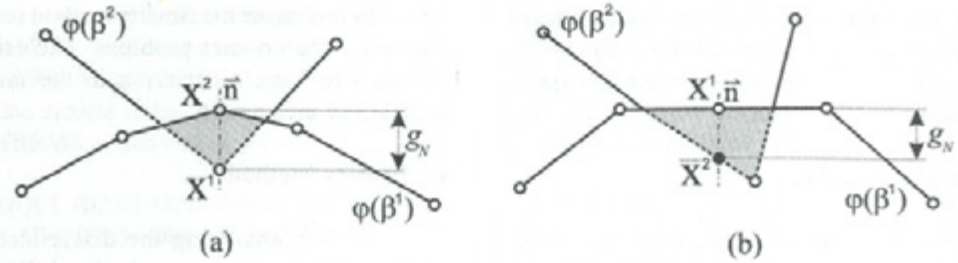

Sl. 8. *Definicija vektorja normale v kontaktni točki: (a)vozlišče - vozlišče, vozlišče - krivulja*
Fig. 8. *Normal vector at the contact point: (a) node-node, node-curve*

$$g_N = \begin{cases} (\overline{\mathbf{X}}^2 - \mathbf{X}^1)\cdot\mathbf{n}^1 & \text{pri pogoju} \quad (\overline{\mathbf{X}}^2 - \mathbf{X}^1)\cdot\mathbf{n}^1 < 0 \\ 0 & \text{pri pogoju} \quad (\overline{\mathbf{X}}^2 - \mathbf{X}^1)\cdot\mathbf{n}^1 \geq 0 \end{cases} \tag{14}$$

kjer je $\mathbf{n}^1$ vektor normale v točki kontakta prodirnega telesa β^1. Ob poznani velikosti in usmerjenosti vektorja prodiranja $\mathbf{g}_N$, lahko normalno kontaktno silo na telo β^1 in β^2 zapišemo kot:

where $\mathbf{n}^1$ represents the normal vector in the contact point of the master body β^1. If the penetration vector $\mathbf{g}_N$ is known, the normal contact force to the master and slave body β^1 in β^2 can be defined as:

$$\mathbf{F}_N^C = \begin{cases} \varphi(\beta^1) & \rightarrow \quad k_N^p \cdot \mathbf{g}_N \\ \varphi(\beta^2) & \rightarrow \quad -k_N^p \cdot \mathbf{g}_N \end{cases} \tag{15}$$

pri čemer k_N^p ponazarja kazenski parameter. Potreben pogoj za konsistenten model kontakta je, da v fazi kontakta ni adhezivnih sil med telesoma. V primeru dodane disipacijske sile v model kontakta, kjer je sila odvisna od usmerjenosti vektorja relativne hitrosti, je le-ta v fazi ekspanzije kontakta adhezivna. Problem lahko rešimo z dodatnim pogojem:

where k_N^p represents the penetration parameter. The necessary condition for the consistent modelling of the contact is that there is no adhesive force during the phase of contact. In the case where an additional damping contact force is considered, the force is dependent on the relative velocity of the bodies in contact, and such an adhesive force can often arise. We can solve this by adding the additional condition

$$D_N^C = \begin{cases} v_N^{rel} \cdot c_N^p, & 0 < t \leq t^k \\ 0, & t^k < t < t^r \end{cases} \tag{16}$$

kjer D_N^C pomeni disipacijsko silo v fazi kontakta, v_N^{rel} relativno hitrost med telesoma v smeri vektorja normale $\mathbf{n}$, t^k pomeni čas od začetka trajanja kontakta do konca faze kompresije kontakta, t^r čas konca faze ekspanzije kontakta in c_N^p disipacijski kazenski parameter. Pogoj (16) je dodan "umetno", saj ni v skladu s fizikalnim modelom kontakta, zato je upoštevan zgolj v fazi numeričnega modeliranja. Končni zapis kontaktne sile C_N je torej:

where D_N^C represents the dissipative force during the phase of contact, v_N^{rel} is the relative velocity of the two bodies in contact in the direction of the contact normal $\mathbf{n}$, t^k is the time from the beginning of the contact to the end of contact compression phase, t^r is the time of the restitution phase and c_N^p is the damping penetration parameter. Condition (16) is considered as artificial, because it has no physical background with regard to the contact model being used. It can only be applied in the numerical phase. The final contact force C_N can be derived as:

$$C_N = k_N^p \cdot \mathbf{g}_N + v_N^{rel} \cdot c_N^p \tag{17}$$

4.1.1 Metoda iskanja kontaktnih točk

Pri izpeljavi algoritma iskanja kontaktnih točk se bomo osredotočili na obravnavan problem jeklene vrvi z oplaščenjem. Obravnavamo problem

4.1.1 The Method For Defining The Contact Points

The searching algorithm is based on the contact problem between the wire and the band. Because the contact points can arise anywhere along the length of

več hkratnih kontaktov, saj do kontakta prihaja med zunanjim premerom jeklene vrvi in notranjim premerom oplaščenja vzdolž osi. Za prodirno telo smo izbrali vrv, tako da je največje število sočasnih točk kontakta definirano s številom vozliščnih točk vzdolž vrvi. Obravnavamo primer poljubno ukrivljene jeklene vrvi z oplaščenjem zato je iskanje mesta kontakta nekoliko bolj zapleteno.

Do kontakta lahko prihaja vzdolž vrvi ter v radialni smeri glede na os vrvi (oplaščenja) (sl. 9).

Ker sta kontaktni meji vrvi in oplaščenja krožnici in če določimo zračnost med vrvjo in oplaščenjem z e, lahko zapišemo pogoj za nastanek kontakta v radialni smeri kot:

$$\mathbf{h} = \mathbf{X}^J - \mathbf{X}^O > e \rightarrow \text{kontakt}$$
$$\mathbf{h} = \mathbf{X}^J - \mathbf{X}^O \leq e \rightarrow \text{ni kontakta} \qquad (18).$$

X^J pomeni vektor pomika prodirnega telesa, X^O vektor pomika predrtega telesa in $\mathbf{h}$ vektor trenutnega odmika med srednjicama obeh teles. S slike 9 je razvidno, da so točke (*i*) srednjica jeklene vrvi, (*ii*) srednjica oplaščenja in (*iii*) kontaktna točka kolinearne.

Določimo prodirno telo z diskretiziracijo M_j končnih elementov. Obstaja torej $M_j + 1$ potencialnih sočasnih mest kontakta z oplaščenjem. Algoritem iskanja kontaktnih točk je takšen, da v vsaki vozliščni točki prodirnega telesa določimo normalno ravnino, nato pa poiščemo morebitno presečišče normalne ravnine s srednjico oplaščenja.

Geometrijska oblika prodirnega telesa je definirana v parametrični obliki kot:

$$\mathbf{R}(s) = \vec{\mathbf{i}}\, x(s) + \vec{\mathbf{j}}\, y(s) + \vec{\mathbf{k}}\, z(s), \quad a < s < b \qquad (19),$$

kjer so $\vec{\mathbf{i}}, \vec{\mathbf{j}}, \vec{\mathbf{k}}$ bazni vektorji kartezičnega koordinatnega sistema, s pa pomeni skalarni

the wire, many simultaneous contacts can arise between the outer diameter of the wire and the inner diameter of the band. Because the wire was chosen to be the master body in contact, the maximum number of simultaneous contacts is defined by the nodal discretization of the wire. The wire and the band can be arbitrarily curved in space, so the searching algorithm to define the contact point can be a little more complicated.

As we mentioned previously, the contact can arise along the wire and in a direction radial to the wire, Figure 9.

Because the contact boundary of the wire and the band are circular functions, and if we defined the gap between the wire and band with e, we can write the condition for the contact to rise in the radial direction as:

where X^J represents the displacement vector of the master body, X^O is the displacement vector of the slave body and $\mathbf{h}$ is the vector of momentary deviation of the two centrelines. It can be seen from Figure 9, that the points on (*i*) the centreline of the wire, (*ii*) centreline of the band and (*iii*) the contact point are collinear.

We can define the master body with M_j finite elements, so the $M_j + 1$ potential contact points between the wire and the band can occur. The algorithm for searching for the contact is based on the fact that we can define the normal contact plane for each node of the master body and find the possible intersection between the normal plane and the centreline of the slave body.

The geometry of the master body can be defined in parametrical form as:

where $\vec{\mathbf{i}}, \vec{\mathbf{j}}, \vec{\mathbf{k}}$ are the base vectors of the Cartesian coordinate system and s is the parametrical

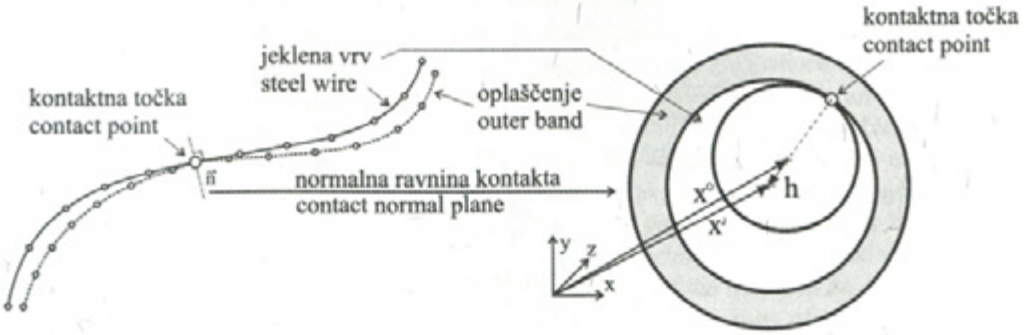

Sl. 9. *Kontaktna točka vzdolž jeklene vrvi v radialni smeri*
Fig. 9. *Contact point along the wire and in a direction radial to the normal plane*

parameter. Po teoriji diferencialne geometrije lahko v vsaki nesingularni točki krivulje določimo ortonormalne bazne vektorje: tangenta $\vec{\mathbf{T}}$, glavna normala $\vec{\mathbf{N}}$ in binormala $\vec{\mathbf{B}}$. V primeru, da poznamo $\mathbf{R}(t)$, $\mathbf{R}'(t)$ in $\mathbf{R}''(t)$, lahko ortonormalne vektorje določimo po enačbah:

parameter. The theory for the differential geometry states that at every non-singular point along the parametrical curve the orthonormal vector can be found: the tangent vector $\vec{\mathbf{T}}$, the principle normal vector $\vec{\mathbf{N}}$ and the binormal vector $\vec{\mathbf{B}}$. If $\mathbf{R}(t)$, $\mathbf{R}'(t)$ and $\mathbf{R}''(t)$ are known, the orthonormal vector can be defined with the equation:

$$\vec{\mathbf{T}} = \frac{\mathbf{R}'(s)}{\|\mathbf{R}'(s)\|}, \quad \vec{\mathbf{B}} = \frac{\mathbf{R}'(s)\times\mathbf{R}''(s)}{\|\mathbf{R}'(s)\times\mathbf{R}''(s)\|}, \quad \vec{\mathbf{N}} = \vec{\mathbf{B}}\times\vec{\mathbf{T}} \tag{20}$$

Glavno normalno ravnino kontakta definirata glavna normala $\vec{\mathbf{N}}$ in binormala $\vec{\mathbf{B}}$. V parametrični obliki lahko zapišemo enačbo ravnine kot:

The principle normal vector $\vec{\mathbf{N}}$ and the binormal vector $\vec{\mathbf{B}}$ define the normal plane in contact. In parametrical form such a plane can be written as:

$$\mathbf{p}_0 + (\mathbf{p}_1 - \mathbf{p}_0)u + (\mathbf{p}_2 - \mathbf{p}_0)v, \quad u, v \in \tag{21}$$

kjer vektor $\mathbf{p}_k = (x_k\, y_k\, z_k)$, $k = 0,1,2$ pomeni tri nekolinearne točke, ki definirajo normalno ravnino, u in v pa pomenita faktorja skaliranja ravnine. Podobno lahko zapišemo parametrično enačbo premice kot:

where $\mathbf{p}_k = (x_k\, y_k\, z_k)$, $k = 0,1,2$ represents three noncollinear points that define the normal plane, u, and v represents the scaling factor of the plane. In the same way we can write the parametrical form for the line:

$$\mathbf{I}_a + (\mathbf{I}_b - \mathbf{I}_a)t, \quad t \in \tag{22}$$

kjer sta $\mathbf{I}_a = (x_a\, y_a\, z_a)$ in $\mathbf{I}_b = (x_b\, y_b\, z_b)$ točki, ki definirata premico. Točko, v kateri premica seka ravnino, lahko zapišemo z enakostjo:

where $\mathbf{I}_a = (x_a\, y_a\, z_a)$ and $\mathbf{I}_b = (x_b\, y_b\, z_b)$ are the line-definition points. The point of intersection between the normal plane and the line can be further calculated from:

$$\mathbf{I}_a + (\mathbf{I}_b - \mathbf{I}_a)t = \mathbf{p}_0 + (\mathbf{p}_1 - \mathbf{p}_0)u + (\mathbf{p}_2 - \mathbf{p}_0)v \tag{23}$$

Rešitev neznanih parametrov t, u in v enačbe (23) predstavlja zapis:

The solution of the unknown parameters t, u and v of Equation (23) can be derived from the equation:

$$\begin{bmatrix} t \\ u \\ v \end{bmatrix} = \begin{bmatrix} x_a - x_b & x_1 - x_0 & x_2 - x_0 \\ y_a - y_b & y_1 - y_0 & y_2 - y_0 \\ z_a - z_b & z_1 - z_0 & z_2 - z_0 \end{bmatrix}^{-1} \begin{bmatrix} x_a - x_0 \\ y_a - y_0 \\ z_a - z_0 \end{bmatrix} \tag{24}$$

Enačba (24) ima v vsakem primeru enolično rešitev. Če je parameter $t \in [0,1]$, je presečišče premice z ravnino med danima točkama $\mathbf{I}_a$ in $\mathbf{I}_b$. V primeru končnih elementov

Equation (24) has only one unique solution. If the parameter $t \in [0,1]$, then the intersection occurs between the given points $\mathbf{I}_a$ and $\mathbf{I}_b$. In the case of finite elements, the points $\mathbf{I}_a$ and $\mathbf{I}_b$ represent

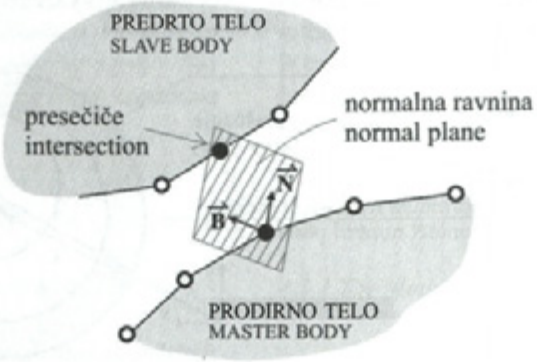

Sl. 10. *Normalna ravnina in točka presečišča s premico*
Fig. 10. *The normal plane and the intersection with the line*

točki $\mathbf{I}_a$ in $\mathbf{I}_b$ predstavljata vozliščne točke enega elementa. Postopek je shematsko prikazan na sliki 10. Ko določimo točko presečišča, lahko po zgornjih enačbah določimo, ali sta telesi v kontaktu ali ne.

4.1.2 Kontaktne sile predrtega telesa

S slike 10 je razvidno, da je prijemališče kontaktne sile na prodirno telo v vozlišču končnega elementa. V primeru predrtega telesa pa lahko kontaktna sila prijemlje v točki po polju elementa, zato je treba določiti ustrezne prispevke kontaktne sile na sosednjih vozliščih končnega elementa. Poznamo transformacijsko matriko elementa $\mathbf{T}_i$. Določeno kontaktno silo na predrto telo lahko v kontaktnem mestu (točka znotraj polja elementa) preoblikujemo iz skupnega v lokalni koordinatni sistem po enačbi:

$$\mathbf{C}_N^L = \mathbf{T}_i^{-1} \cdot \mathbf{C}_N^G \tag{25},$$

kjer $\mathbf{C}_N^L$ pomeni komponente kontaktne sile prediranega telesa v lokalnem koordinatnem sistemu elementa, $\mathbf{C}_N^G$ pa komponente v skupnem koordinatnem sistemu. Če določimo interpolacijsko matriko končnega elementa kot $\mathbf{N}_i$, lahko zapišemo vozliščne vrednosti kontaktne sile kot:

$$\bar{\mathbf{C}}_{N(i)} = \sum_{i=1}^{n} \mathbf{N}_i \, \mathbf{C}_{N(i)}^L \tag{26}.$$

Indeks i pomeni i-to prostostno stopnjo elementa oziroma i-ti interpolacijski polinom.

4.1.3 Integracija gibalnih enačb

V prvem delu prispevka, ko obravnavamo prenos vibracij po jekleni vrvi brez oplaščenja, smo se osredotočili samo na odziv v ustaljenem stanju. Ker je sistem linearen, je reševanje takšnega sistema razmeroma preprosto, enačbi (6) in (7). Pri obravnavi kontaktnega problema med vrvjo in oplaščenjem dinamični sistem postane nelinearen. Numerične metode v splošnem ponujajo veliko integracijskih metod, v našem primeru smo uporabili Newmarkovo integracijsko metodo [11]. Metoda predpostavlja, da je sprememba pospeška med dvema časovnima trenutkoma linearna. Razlog za izbiro te metode je v tem, da je stabilnost metode neodvisna od velikosti časovnega koraka Δt.
Rešujemo diferencialno enačbo oblike:

the nodal points of the element. The process is schematically shown in Figure 10. After defining the intersection points and by using the contact conditions, one can detect when the two bodies come into contact.

4.1.2 The Contact Force of the Slave Body

We can see from Figure 10 that the contact force on the master body is at the nodal point, but in the case of the slave body the contact force can be somewhere along the finite element. For this reason the proper contact-force components must be defined and applied to the neighbouring nodes. If the transformation matrix $\mathbf{T}_i$ of the finite element is known, the contact force can be first transformed from the global coordinate system into the local coordinate system of the element by

$$\mathbf{C}_N^L = \mathbf{T}_i^{-1} \cdot \mathbf{C}_N^G \tag{25},$$

where $\mathbf{C}_N^L$ represents the contact-force component of the slave body in the local coordinate system of the element and $\mathbf{C}_N^G$ the components in the global coordinate system. If we define the interpolation matrix of the element $\mathbf{N}_i$, the nodal components of the contact force can be computed from Equation (26):

$$\bar{\mathbf{C}}_{N(i)} = \sum_{i=1}^{n} \mathbf{N}_i \, \mathbf{C}_{N(i)}^L \tag{26}.$$

Index i represents the i-th element degree of freedom with the i-th interpolation polynomial.

4.1.3 Integration of the Equations

In the first part of the paper, when only the vibration transmission over the wire was considered, we focused only on the steady-state response. Because the system was linear, the solution of the equations of motion was relatively easy to define, Equations (6) and (7). However, when the contact is considered in the equations of motion, the problem becomes nonlinear. There are many integration routines for solving such a problem. In our case we used the Newmark integration method [11]. The method assumes that the change in acceleration between two time instances is linear. The main reason for choosing this method was its insensitivity to the size of the time step Δt.
We solve the equation of motion:

$$\mathbf{M}\ddot{\mathbf{x}} + \mathbf{C}\dot{\mathbf{x}} + \mathbf{K}\mathbf{x} = \mathbf{F}_z + \mathbf{F}_g + \mathbf{C}_N \tag{27},$$

kjer vektor $\mathbf{F}_z$ pomeni zunanje obremenitve, vektor $\mathbf{F}_g$ težnostno silo in vektor $\mathbf{C}_N$ kontaktne sile sistema, enačba (17). Zapisana enačba predstavlja enačbo gibanja prodirnega telesa. V primeru predrtega telesa je zapis gibalne enačbe enak, ustrezno je spremenjena le velikost in usmerjenost vektorja kontaktnih sil $\mathbf{C}_N$.

Predpostavimo, da poznamo vrednosti vektorja pomikov, hitrosti in pospeškov sistema v času t_i. V [10] je prikazana podrobnejša izpeljava Newmarkove metode, zato bomo v nadaljevanju z vidika celovitosti prispevka zapisali končne enačbe za izračun vektorja pomika, vektorja hitrosti in vektorja pospeška pri času t_{i+1}. Vektor pomika zapišemo kot:

where $\mathbf{F}_z$ is the vector of external forces, $\mathbf{F}_g$ the vector of gravitational force and $\mathbf{C}_N$ the contact force, Equation (17). Equation (27) represents the equation of motion for the master body. In the case of the slave body, the equation is practically the same; the only change is in the vector of the contact forces, where the proper direction and values need to be adopted.

We can assume that the displacement, the velocity and the acceleration amplitudes of the system are know at instance t_i. In [11] a detailed construction of the Newmark method is presented, so here only the final equations are presented. The displacement vector of the system at instance t_{i+1} can be computed from

$$\mathbf{x}_{i+1} = \left[\frac{1}{\kappa(\Delta t)^2}\mathbf{M} + \frac{\lambda}{\kappa\,\Delta t}\mathbf{C} + \mathbf{K}\right]^{-1} \cdot \left\{\mathbf{F}_{i+1} + \mathbf{M}\left(\frac{1}{\kappa(\Delta t)^2}\mathbf{x}_i + \frac{\lambda}{\kappa\,\Delta t}\dot{\mathbf{x}}_i + \left(\frac{1}{2\kappa} - 1\right)\ddot{\mathbf{x}}_i\right)\right.$$
$$\left. + \mathbf{C}\left(\frac{\lambda}{\kappa\,\Delta t}\mathbf{x}_i + \left(\frac{\lambda}{\kappa} - 1\right)\dot{\mathbf{x}}_i + \left(\frac{\lambda}{\kappa} - 2\right)\frac{\Delta t}{2}\ddot{\mathbf{x}}_i\right)\right\} \tag{28},$$

vektor pospeška kot:

the acceleration vector as:

$$\ddot{\mathbf{x}}_{i+1} = \frac{1}{\kappa(\Delta t)^2}\left(\mathbf{x}_{i+1} - \mathbf{x}_i\right) - \frac{1}{\kappa\,\Delta t}\dot{\mathbf{x}}_i - \left(\frac{1}{2\kappa} - 1\right)\ddot{\mathbf{x}}_i \tag{29}$$

in vektor hitrosti kot:

and the velocity vector as:

$$\dot{\mathbf{x}}_{i+1} = \dot{\mathbf{x}}_i + (1-\lambda)\Delta t\,\ddot{\mathbf{x}}_i + \lambda\,\Delta t\;\ddot{\mathbf{x}}_{i+1} \tag{30}.$$

Pri izbiri parametrov κ in λ je pomembna predvsem izbira parametra b. V primeru ko je $\lambda \neq 0{,}5$, vnesemo v integracijo umetno dušenje. V našem primeru sta bila parametra enaka $\kappa = 0{,}25$ in $\lambda = 0{,}5$.

V primeru, ko kontaktov ne obravnavamo, je časovni korak ves čas integracije stalen. Ko pride do kontaktov, je treba za natančnejše rezultate integracije časovni korak v času kontakta ustrezno zmanjšati. V numeričnem preizkusu smo upoštevali, da se časovni korak v času kontakta zmanjša na $\Delta t_c = \Delta t/5$.

The important thing is the choice of the proper parameters κ and λ in Equations (28) to (30). The parameter b is important, because if the $\lambda \neq 0.5$, then spurious damping is introduced into the system. In our case the values were $\kappa = 0.25$ and $\lambda = 0.5$.

In the case where the contacts are not identified, the time step can be made constant during the integration. However, when the contacts arise the time step must be made smaller. In the numerical simulation, the time step when there was no contact was Δt_c, and when the contact was identified the time step was changed to $\Delta t_c = \Delta t/5$.

5 NUMERIČNI PREIZKUS

Poglavje je namenjeno numeričnemu preizkusu dinamičnega obnašanja jeklene vrvi skupaj z oplaščenjem ob upoštevanju vmesnega kontakta. V poglavju 5.1 je predstavljen numerični preizkus ukrivljene jeklene vrvi v prostoru, pri čemer smo opazovali morebitne spremembe v odzivu sistema pri spremembi zgolj velikost zračnosti med vrvjo in oplaščenjem.

5 NUMERICAL SIMULATION

In this section the numerical simulation of the dynamical behaviour of the wire with the band and the interaction contact will be given. In section 5.1 the simulation of the dynamic transmission over the curved wire and the band will be shown. The possible changes in the response due to different values of the gap will be described.

V poglavju 5.2 bo predstavljen primer uporabe t.i. mehanskega filtra. Namen mehanskega filtra je znižati raven vibracij oziroma znižati resonančne vrhove strukture. Parametra togosti in dušenja v modelu kontakta sta v vseh primerih numeričnega preizkusa konstantna, in sicer $k_N^p = 10^5$ N/m in $c_N^p = 100$ Ns/m.

5.1 Numerični preizkus prenosa vibracij po jekleni vrvi in oplaščenja

V tem poglavju je predstavljen numerični preizkus prenosa vibracij preko jeklene vrvi z oplaščenjem, pri čemer spreminjamo zgolj vrednost zračnosti. V preglednici 2 so podane vrednosti parametrov numeričnega preizkusa. Prikazana bo zgolj funkcija TRFAM za kontaktni primer pri dveh različnih zračnostih med vrvjo in oplaščenjem za smer sile v podpori z. Vzbujevalni signal je naključen v območju frekvenc od 10 Hz do 1000 Hz, RMS = 20 ms^{-2} (RMS - efektivna vrednost signala)

Geometrijska oblika jeklene vrvi in oplaščenja je enaka kakor v primeru v poglavju 3. Vrv in oplaščenje sta bila diskretizirana s 30 končnimi elementi.

In section 5.2 the use of the mechanical filter will be demonstrated. The main purpose of the mechanical filter is to minimize the vibration transmission or to minimize the resonance peaks of the structures. The stiffness and damping-contact parameters were set to be constant during all the numerical simulations, i.e., $k_N^p = 10^5$ N/m and $c_N^p = 100$ Ns/m.

5.1 Simulation of the Vibration Transmission over the Wire with the Band

In this section the numerical simulation of the vibration transmission over the wire with the band will be shown. The only parameter that was varied during the simulation was the gap size. In Table 2 the values used for each simulation are shown, while all the other parameters can be seen from Table 1. The TRFAM function for the contact problem with a different gap value will be shown. The simulated measured direction of the support force is z. The excitation signal was random between 10 Hz and 1000 Hz, RMS = 20 ms^{-2}.

The geometry of the wire and the band was adopted from Section 3. The number of finite elements used for the wire and the band was 30.

Preglednica 2. *Parametri pri različnih numeričnih preizkusih*
Table 2. *Parameters for different numerical simulations*

Preizkus *Simulation*	*Dinamični modul elastičnosti oplaščenja – E* [Nm^2] *Dynamic modulus od elasticity of outer band – E* [Nm^2]	*Zračnost - e* [m] *Gap - e* [m]
1. – Sl., Fig (10)	*60 GPa*	$1{,}5 \cdot 10^{-4}$
2. – Sl., Fig (10)	*60 GPa*	$6{,}5 \cdot 10^{-4}$

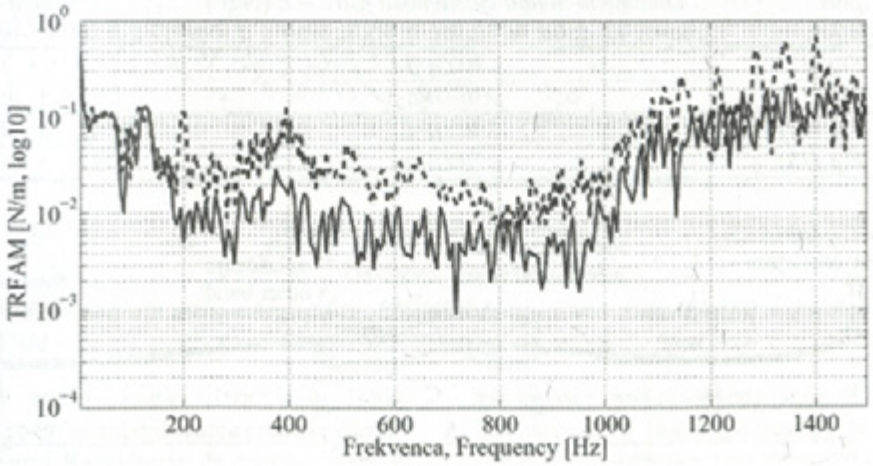

Sl. 10. *TRFAM jeklene vrvi in oplaščenja: zračnost (—) e=1,5 · 10^{-4} m in (- -) e=6,5 · 10^{-4} m*
Fig. 10. *TRFAM of the wire and the band: gap (—) e=1.5 · 10^{-4} m and (- -) e=6.5 · 10^{-4} m*

S slike 10 je razvidno, da ima velikost zračnosti vpliv na spremembo prenosa vibracij po jekleni vrvi z oplaščenjem predvsem v višjem frekvenčnem področju. Večja zračnost nekoliko poviša prenos vibracij.

5.2 Uporaba mehanskega filtra

Za ocenitev uporabnosti mehanskega filtra smo uporabili funkcijo TRFAM, enačba (8). Na sliki 11 je prikazan primer uporabe mehanskega filtra. Zasledovali smo dva parametra, in sicer kako na prenos vibracij vpliva togost mehanskega filtra ter velikost zračnosti e med vrvjo in mehanskim filtrom. Geometrijski podatki vrvi in oplaščenja so podani v preglednici 1.

Vzbujevalni signal je sinusni signal s preletom frekvenc od *10* Hz do *1000* Hz. Amplituda vzbujevalnega pospeška je *100* ms^{-2} in je v vseh primerih enaka. Vrednosti položajnih parametrov mehanskega filtra so: A = *321* mm, B = *120* mm in C = *60* mm. Jeklena vrv je bila diskretizirana s 25 končnimi elementi, mehanski filter pa s16 končnimi elementi.

Preglednica 3 prikazuje vrednosti dinamičnega modula elastičnosti in zračnosti pri posameznih preizkusih. V preglednici so označene tudi številke slik, ki pripadajo rezultatu preizkusa.

Rezultati numeričnih preizkusov na slikah 12, 13, 14 in 15 nakazujejo, da je pri izbiri ustreznih

It is clear from Figure 10 that the gap size has a significant influence on the change of the vibration transmission over the wire with the band mostly in the high frequency region. The larger gap size produces a higher vibration transmission.

5.2 The Use of the Mechanical Filter

For the estimation of the quality of the mechanical filter the TRFAM function was computed, Equation (8). Figure (11) shows the example of the mechanical filter. We investigated how the stiffness and the gap size between the wire and the band influenced the vibration transmission. The geometrical properties for the wire and the band are listed in Table 1.

The excitation signal was a chirp sine from a frequency of *10* Hz to one of *1000* Hz. The acceleration amplitude was *100* ms^{-2}, and this was kept the same for all the numerical simulations. The values of the position parameters of the filter were: A = *321* mm, B = *120* mm and C = *60* mm. The wire was discretized with the 25 finite elements, and the mechanical filter with 16 finite elements.

Table 3 shows the values of the parameters that were changed during each simulation. The table also includes the figure numbers of the results.

The results in Figures 12, 13, 14 and 15 show that the mechanical filter, with the properly chosen parameters, can significantly lower the vibration

Preglednica 3. *Parametri pri različnih numeričnih preizkusih*
Table 3. *Parameters for different numerical simulations*

Preizkus *Simulation*	*Dinamični modul elastičnosti filtra – E* [Nm^2] *Dynamic modulus od elasticity of the filter – E* [Nm^2]	*Zračnost - e* [m] *Gap - e* [m]
1. – Sl., Fig (12)	*30 GPa*	$6{,}5 \cdot 10^{-4}$
2. – Sl., Fig (13)	*30 GPa*	$5 \cdot 10^{-5}$
3. – Sl., Fig (14)	*50 GPa*	$5 \cdot 10^{-5}$
4. – Sl., Fig (15)	*70 GPa*	$5 \cdot 10^{-5}$

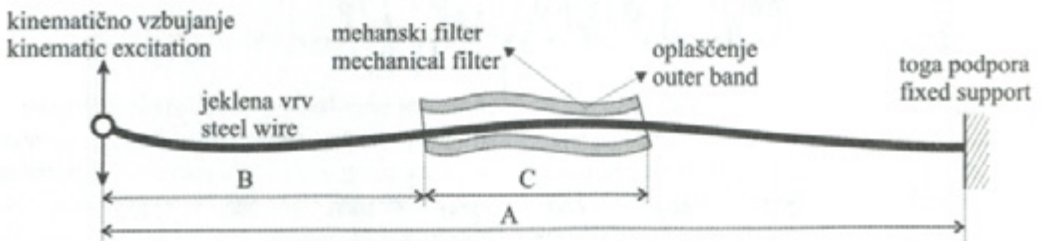

Sl. 11. *Primer uporabe mehanskega filtra*
Fig. 11. *Example of using the mechanical filter*

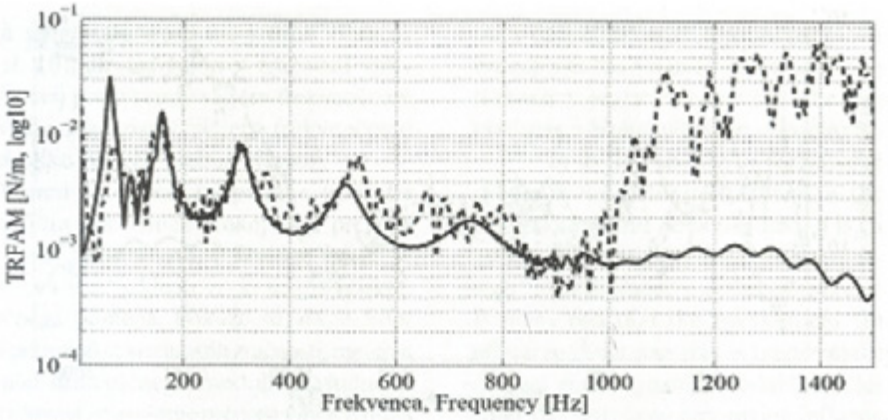

Sl. 12. *TRFAM pri uporabi mehanskega filtra, PRIMER 1; (—) brez meh. filtra, (- -) z meh. filtrom*
Fig. 12. *TRFAM with the mechanical filter, CASE 1; (—) without mech. filter, (- -) with mech. filter*

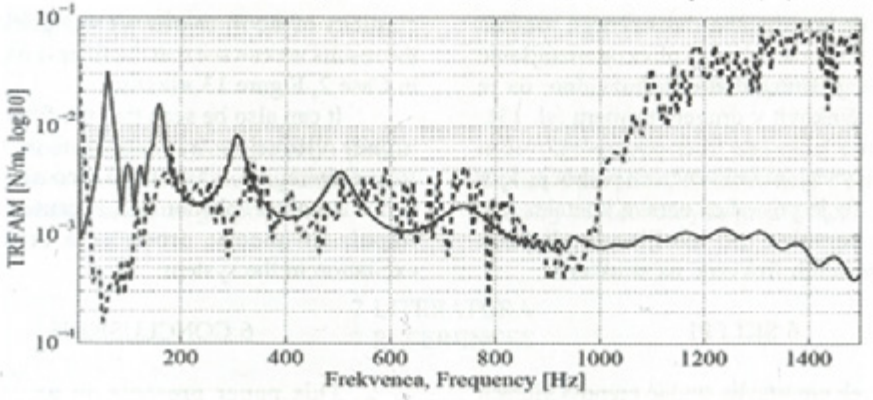

Sl. 13. *TRFAM pri uporabi mehanskega filtra, PRIMER 2; (—) brez meh. filtra, (- - -) z meh. filtrom*
Fig. 13. *TRFAM with the mechanical filter, CASE 2; (—) without mech. filter, (- -) with mech. filter*

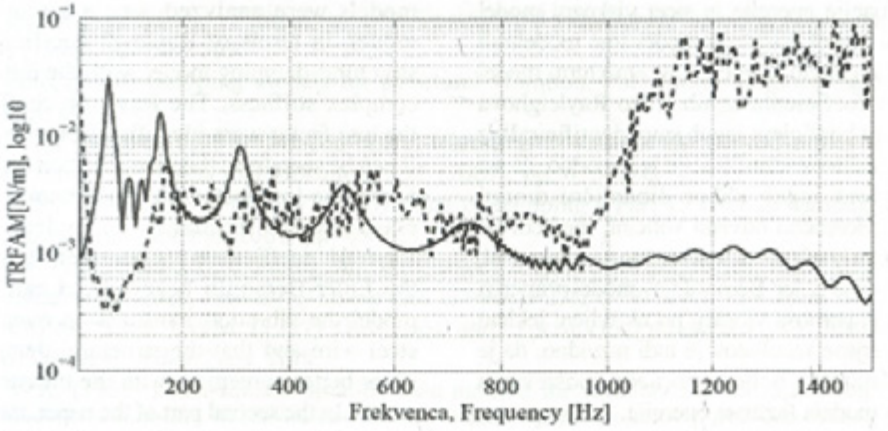

Sl. 14. *TRFAM pri uporabi mehanskega filtra, PRIMER 3; (—) brez meh. filtra, (- - -) z meh. filtrom*
Fig. 14. *TRFAM with the mechanical filter, CASE 3; (—) without mech. filter, (- -) with mech. filter*

parametrov mehanskega filtra le-ta lahko učinkovito orodje za zmanjševanje prenosa vibracij prek jeklene vrvi. Razvidno je, da velikost zračnosti med jekleno vrvjo in mehanskim filtrom pomembno vpliva na prenos vibracij. Prav tako lahko

transmission and resonance peaks of the structure. The parameter that significantly influences the vibration transmission was shown to be the size of the gap between the wire and the band. We can also see that the influence of the dynamic modulus of

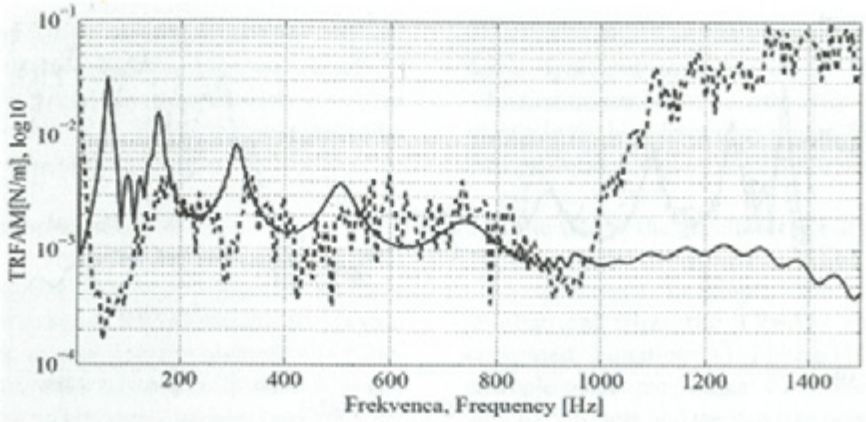

Sl. 15. *TRFAM pri uporabi mehanskega filtra, PRIMER 4; (—) brez meh. filtra, (- - -) z meh. filtrom*
Fig. 15. *TRFAM with the mechanical filter, CASE 4; (—) without mech. filter, (- -) with mech. filter*

povzamemo, da sprememba dinamičnega modula elastičnosti filtra nima večjega vpliva na zmanjšanje prenosa vibracij. Iz rezultatov je razvidno, da je filter najbolj učinkovit v drugem primeru (sl. 13).

Opazimo lahko, da filter povzroči povečan prenos vibracij v višjem frekvenčnem področju, kjer ni vzbujanja. To je posledica narave kontakta, saj vsak impulz kontakta (po teoriji) vzbudi širok spekter vzbujevalnih frekvenc na strukturo.

6 SKLEPI

Prispevek predstavlja študijo prenosa vibracij po poljubno ukrivljeni jekleni vrvi, ki je v osni smeri neobremenjena. Analizirana sta bila dva različna modela disipacije energije in sicer viskozni model ter strukturni model. Viskozni model smo modelirali v obliki Rayleighovih koeficientov, strukturni model pa z uvedbo koeficienta izgub. Tako Rayleighova koeficienta kot koeficient izgub smo identificirali iz meritev. Iz rezultatov idntifikacije je razvidno, da sta tako koeficient izgub kakor dinamični modul elastičnosti frekvenčno odvisni veličini, medtem ko sta Rayleighova koeficienta frekvenčno neodvisna (sl. 5). Izkaže se, da je Euler-Bernoullijev model primeren za modeliranje prenosa vibracij po ukrivljeni jekleni vrvi. Iz primerjave rezultatov je tudi razvidno, da je ujemanje rezultatov bolje v primeru upoštevanja strukturnega modela raztrosa energije.

V drugem delu prispevka je prikazana obravnava jeklene vrvi z oplaščenjem, pri čemer je medsebojni kontakt obravnavan po kazenski metodi. Iskanje mesta kontakta je prevedeno na iskanje presečišča med normalno ravnino v izbranem vozlišču prodirnega telesa in premico, ki je srednjica končnega elementa prodiranega telesa. Narejen je bil numerični preizkus za ovrednotenje

elasticity of the filter was not so significant. From the results we can see that the filter is most effective in Case 2, Figure 13.

It can also be seen that the filter produces a higher vibration transmission in the higher frequency region, where there is no excitation. This is due to contact phenomena, because each contact impuls, in theory, produces a broad band of excitation in the system.

6 CONCLUSIONS

This paper presents an analysis of the vibration transmission over an arbitrary curved steel wire with no axial pre-load. Two different damping models were analyzed, i.e., a viscous-damping model, in terms of Rayleigh coefficients, and a structural-damping model, with the introduction of complex stiffness. The Rayleigh coefficients and the loss factor were identified from measurements. It can be seen from the identification results, Figure 5, that the loss factor and the dynamic modulus of elasticity are frequency dependent, while the Rayleigh coefficients are constant. It turns out that the Euler-Bernoulli beam model can be used to model the vibration transmission over the curved steel wire and that the structural damping model gives better agreement with the measured results.

In the second part of the paper, the analysis of the steel wire with an outer band is presented, where the contact between them is modelled using the penalty method. The search for the contact point is transferred to a search for the intersection point between the normal contact plane of the master body node with the line segment of the slave body. A numerical simulation was made to analyze the influence of the gap size on the vibration transmission, while all the

morebitnega vpliva zračnosti na prenos vibracij. Pokaže se (sl. 10), da ima velikost zračnosti vpliv na prenos vibracij predvsem v višjem frekvenčnem področju. Večja zračnost v višjem frekvenčnem področju nekoliko poveča prenos vibracij.

Na koncu je prikazan primer uporabe mehanskega filtra za namen zmanjšanja prenosa vibracij po ravni jekleni vrvi. Razvidno je, da je velikost zračnosti med jekleno vrvjo in mehanskim filtrom ključnega pomena. Pokaže se, da je filter učinkovitejši pri manjših vrednostih zračnosti, medtem ko sprememba dinamičnega modula elastičnosti mehanskega filtra na zmanjšanje prenosa vibracij nima večjega vpliva. Poudariti je treba, da so bile geometrijske in položajne vrednosti mehanskega filtra v vseh numeričnih preizkusih konstantne.

other parameters were kept constant. We showed that the gap size has a significant value, mostly in the high-frequency region, Figure 10. The larger gap size produces a higher vibration transmission.

In the last section of the paper the use of the mechanical filter to minimise the vibration transmission was demonstrated. It is clear from the numerical simulations that the gap size has a significant influence on the vibration transmission. It turns out that the mechanical filter is more effective if the gap size is made smaller, while the change in the dynamic modulus of elasticity of the filter did not show any major influence. It should be pointed out that the geometrical and positional properties of the mechanical filter were kept constant between the numerical simulations.

Zahvala

Za pomoč se zahvaljujemo podjetju Cimos d.d., Ministrstvu za visoko šolstvo, znanost in tehnologijo in Ministrstvu za gospodarstvo.

Acknowledgement

The support of Cimos d.d., Ministry of Higher Education, Science and Technology and Ministry of Economy is greatly acknowledged.

7 LITERATURA
7 REFERENCES

[1] G.A. Costello (1990) Theory of wire rope, *Springer*, Berlin.
[2] A. Nawrocki, M. Labrosse (2000) A finite element model for simple straight wire rope strands, *Computers and Structures*, 77, (2000), pp. 345–359.
[3] J. Woodhouse (1998) Linear damping models for structural vibrations, *Journal of Sound and Vibration*, 215 (3), (1998), pp. 547–569.
[4] S. Adhikari (2000) Damping models for structural vibration, PhD thesis, Engineering Department, *Cambridge University*.
[5] M. Otrin, M. Boltežar (2007) Damped lateral vibrations of straight and curved cables with no axial pre-load, *Journal of Sound and Vibration*, 300, (2007), pp. 676-694.
[6] Adhikari S., Woodhouse J. (2001) Identification of damping - Part 1: viscous damping, *Journal of sound and vibration*,243(1), 2001, pp. 43–61.
[7] Bert, C.W. (1973) Material damping: an introductory review of mathematical models, measures and experimental techniques, *Journal of sound and vibration* 29(2), 1973, pp. 129–153.
[8] Maia, N.M.M., Silva, J.M.M. (1997) Theoretical and experimental modal analysis, Instituto Superior Téhnico, Portugal, *Wiley*, New York.
[9] Smith, W.R. (1981) Least-squares time-domain method for simultaneous identification of vibration parameters from multiple free-response record, *American Institute of Aeronautics and Astronautics, Inc.*, California, pp. 194–201.
[10] Peter Wriggers (2002) Computational contact mechanics, *Wiley cop.*
[11] S. S. Rao (1995) Mechanical vibrations, *Purdue University*.

Naslov avtorjev: Miha Otrin
Cimos d.d.
Cesta Marežganskega upora 2
6000 Koper
miha.otrin@fs.uni-lj.si

prof. dr. Miha Boltežar
Univerza v Ljubljani
Fakulteta za strojništvo
Aškerčeva 6
1000 Ljubljana
miha.boltezar@fs.uni-lj.si

Authors' Address: Miha Otrin
Cimos Ltd.
Cesta Marežganskega upora 2
SI-6000 Koper, Slovenia
miha.otrin@fs.uni-lj.si

Prof. Dr. Miha Boltežar
University of Ljubljana
Faculty of Mechanical Eng.
Aškerčeva 6
SI-1000 Ljubljana, Slovenia
miha.boltezar@fs.uni-lj.si

Prejeto: 23.7.2007
Received:
Sprejeto: 28.9.2007
Accepted:
Odprto za diskusijo: 1 leto
Open for discussion: 1 year